

# Development of MRI-Powered Modular Robotic System

Ryutaro Ouchi<sup>1</sup>, Kousaku Saotome<sup>2</sup>, Akira Matsushita<sup>3</sup> and Kenji Suzuki<sup>4</sup>

**Abstract**—This study proposes a novel robotic system controlled by the magnetic forces generated from Magnetic Resonance Imaging (MRI) scanner. In the proposed system, ferromagnetic particles are used to actuate the device, while all other parts are made of nonmagnetic materials. The possible range of motion for the particles is investigated by using the common sequence which is usually available for MR imaging. We then designed a mechanism that extends the observed pendular motion to rotational movement. By using the designed mechanism, we realized a MRI-powered multiaxial robotic system. The potential application of this system covers the automation for under MRI inspections such as esthesiometry and needle biopsy. In this paper, we described the fundamental principle of the MRI-powered robotic system and also report on the performance evaluation of the robotic system.

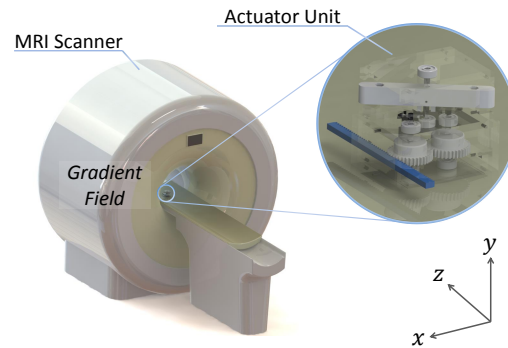


Fig. 1. System Overview

## I. INTRODUCTION

In recent years, the use of magnetically driven devices have been progressing in the medical field [1][2]. The advantage of these devices is that it is possible to activate the machine or sense the object without any physical contacts. For example, motion capture system using magnetostrictive vibration [3] and endoscope using magnetic field [4] have been developed.

Magnetic Resonance Imaging (MRI) is a medical imaging technique used to investigate the anatomy and function inside the body. MRI scanner contains electromagnets, constantly emitting strong magnetic field around the scanner. However, since the MRI delivers high amounts of electromagnetic energy, the use of devices containing magnetic materials is strictly restricted inside the MRI room.

Several MR-compatible systems are being developed to overcome these problems [5][6][7]. These systems usually consist of three parts: actuator, controller and operation unit. In many cases, the first two parts contain magnetic materials, so that they should be installed outside of the MRI room and only power is transmitted inside the room. To achieve this efforts and modifications of the MRI room are needed such as making holes in the magnetic shielding wall. Thus, the existing MR-compatible systems often become problematic

\*This study was supported by the "Funding Program for World-Leading Innovative R&D on Science and Technology" (FIRST Program)

<sup>1</sup>Ryutaro Ouchi is with the Graduate School of Systems and Information Engineering, University of Tsukuba, Japan ryutaro at ai.iit.tsukuba.ac.jp

<sup>2</sup>Kousaku Saotome is with the Center for Cybernics Research, University of Tsukuba, Japan saotome at ccr.tsukuba.ac.jp

<sup>3</sup>Akira Matsushita is with the Center for Cybernics Research, University of Tsukuba, Japan akira at ccr.tsukuba.ac.jp

<sup>4</sup>Kenji Suzuki is with Faculty of Engineering, Systems and Informatics, and the Center for Cybernics Research, University of Tsukuba, Japan kenji at ieee.org

for the practical use when the mechanism become highly complicated.

In this study, we introduce a multiaxial robotic system actuated and controlled by the magnetic field generated from MRI scanner.

Recent studies made by Dupont et al. [8][9][10] have investigated the possibility of MRI-powered actuator. In these studies, they realized an actuator of uniaxial oscillating rotary movement by using the sequence originally made for activating the actuator. On the other hand, the robotic system we suppose as illustrated in Fig. 1 realizes multiaxial movement with the existing imaging sequence. The developed modular robotic system can be assembled for different purposes solely by connecting the mechanical shafts with mechanical joints.

## II. ACTUATION TECHNOLOGY

### A. Gradient Field

The principle of actuation is based on a ferromagnetic particle embedded in the rotor that serves to convert the electromagnetic forces from the MR gradients into mechanical energy. Gradient magnetic field are generally divided into the following: slice-selective gradient, phase-encoding gradient, and readout gradient. Among these three types of gradient magnetic field, slice-selective gradient generates the most powerful gradient field. Activation of the actuator using magnetic field of MRI is realized by controlling the timing and intensity of the slice-selective gradient magnetic field.

### B. Force Model

Fig. 2 shows the schematic diagram of the force with regard to the ferromagnetic body when it is inserted into the magnetic field. When a ferromagnetic material is inserted into the gradient magnetic field, north pole and south pole will appear on both ends of the material. The force applied

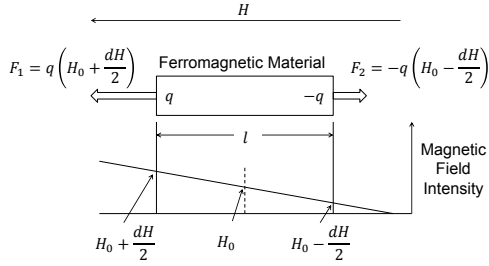


Fig. 2. Force Model

to the north and south pole are denoted  $q(H_0 + dH/2)$  [N], and  $q(H_0 - dH/2)$  [N] where  $q$  [Wb] is the intensity of the magnetic pole and  $H$  is intensity of the magnetic field. Thus, the force applied to the whole ferromagnetic body is described as:

$$F = q \cdot dH \quad (1)$$

The intensity of the magnetic pole  $q$  is also described as:

$$q = \frac{V\mu_0\chi H_0}{dl} \quad (2)$$

where  $V$  [m<sup>3</sup>] is the volume of the magnetic body,  $\mu_0$  is the vacuum permeability, and  $\chi H_0$  [kA/m] is the magnetic susceptibility. By assigning  $q$  and the equation of magnetic flux density,  $B = \mu_0 H$ , into equation (1), we came with the following expression:

$$F = V \frac{\chi}{\mu_0} B \frac{dB}{dl} \quad (3)$$

The developed robotic system works by generating torque based on this force. The torque can be generated by moving the ferromagnetic particle embedded at a certain radius  $r$  [m] from the rotating shaft of the mechanism. The generated torque  $T$  [N·m] is given by:

$$T = V \frac{\chi}{\mu_0} B \frac{dB}{dl} r \sin \theta \quad (4)$$

where  $\theta$  is the angle formed by the rotor and the direction of the gradient field.

### III. SYSTEM OVERVIEW

The robotic system is composed of MRI scanner, a computer for controlling the MRI scanner and actuator units. The operator first transmits the sequence to MRI scanner and it starts to generate gradient field. Under the effect of the gradient field, the rotor incorporated in the robotic system will start a pendulum movement. The developed mechanism inside the actuator unit converts the pendulum movement to one-way rotation considered as the output.

#### A. MRI Scanner and Sequence

MRI scanner used in this study is Achieva 3.0T TX (Royal Philips). Its maximum gradient field is 80 mT/m and maximum slew rate is 200 mT/m/ms. The diameter of the MRI gantry is 60 cm.

The sequence used for the robotic system is Turbo Spin Echo (TSE), which is one of the common imaging sequences

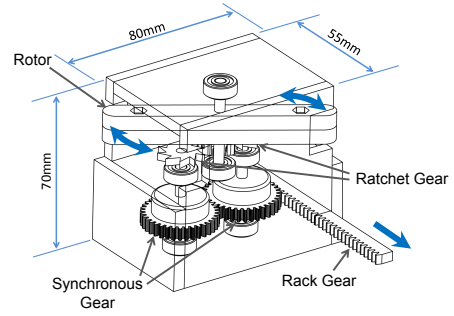


Fig. 3. Actuator Unit

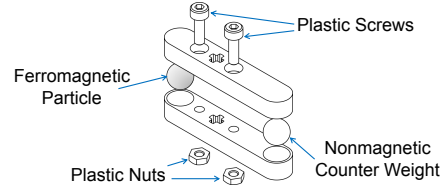


Fig. 4. Construction of the Rotor

and typically used for clinical examinations. To make the slice-selective magnetic field gradient stronger, several parameters such as slice thickness, echo time, repetition time, and turbo factor should be adjusted. We considered it as a feasible sequence to activate the actuator because the adjustment range of these parameters in TSE is wider compared to other sequences.

#### B. Actuator Unit

Fig. 3 shows the general view of the actuator unit. This unit consists of the rotor and the conversion mechanism.

1) *Rotor*: The construction of the rotor is illustrated in Fig. 4. A ferromagnetic sphere attached in the rotor is used to generate the driving torque. The material of the sphere is chrome steel (SUS304), often used for ball bearing, with a diameter of 8 mm.

The proposed robotic system aims to achieve multiaxial movement. One possible approach for this is to use multiple independent planes to rotate rotors (e.g.  $x$ - $y$  and  $x$ - $z$  planes). In the case of uniaxial movement the mechanism can be designed without the need for a weight balanced rotor, but in the case of multiaxial movement a weight balanced rotor is needed. Therefore, we loaded the rotor with a counter weight against the ferromagnetic part. Since it is difficult to find nonmagnetic materials which has same density as chrome steel, we made one side of the rotor longer than the other side to balance the weight.

2) *Mechanism*: The mechanism shown in Fig. 5(a) converts the pendulum movement to one-way rotation, which is constructed from a rotor, synchronous gears and ratchet gears.

Synchronous gears and ratchet gears on the left and right side of the rotor are connected and rotate together. Two ratchet gears are set up half-cycle shifted, which enables the rotor to always touch both cogs of the two gears. When the rotor pushes the ratchet gear on one side, the synchronous gear also rotates, making the ratchet gear on the

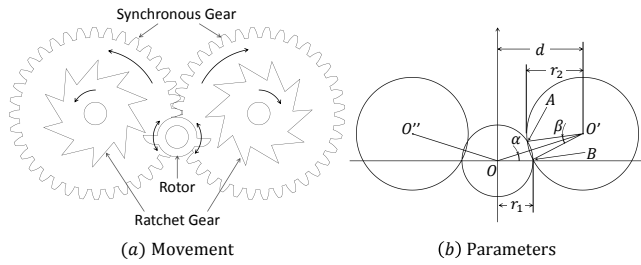


Fig. 5. Movement and Parameters of the Conversion Mechanism

other side reach to the contact point again, and thus making continuous motion. In this way, the proposed mechanism converts pendulum movement to one-way rotation.

Fig. 5(b) shows the gear parameters for proper design of the mechanism to achieve the desired function. The circle which center point is the origin  $O$  represents the rotor, and the two circles on both sides of the rotor are the periphery of the ratchet gears.

The important factors in this design are the radius of the rotor  $r_1$ , the radius of the ratchet gear  $r_2$ , and their relative positions. This mechanism should fulfill two conditions to function properly:

- 1) The circle of the rotor and the ratchet gear intersect in two points
- 2) Intersection points  $A$  and  $B$  are in the motion range of the rotor

To generate one-way rotation by using this mechanism, we carefully selected the motion range of the rotor that matches to these two conditions. By embedding this mechanism to the robotic system, we could achieve rotary motion using magnetic energy of the MRI sequence.

#### IV. PERFORMANCE EVALUATIONS

We conducted the experiments to verify the performance of the developed robotic system. When the MRI scanner is under operation, it generates small vibrations from the imaging process, and this can affect rotation of the rotor. Therefore, the rotor should be settled completely parallel to ground in order to obtain high accuracy results. To achieve this, we used a nonmagnetic level gauge and acrylic board to make sure the system lays on flat surface.

Also, to use the MRI scanner, there should be an object that emits hydrogen-like signals inside the gantry. The developed robotic system is constructed with resin, plastic materials and one ferromagnetic sphere, so the scanner do not get any signals from the device. Thus, "Phantom", a material able to transmit the signals and usually used for maintenance of the scanner, was used.

##### A. Rotation Angle Measurement

We devised this experiment to evaluate the motion range of the rotor for developing the mechanism explained in section III-B.2.

The blue area of the graph illustrated in Fig. 6 shows the region on which the rotor is able to realize the pendulum

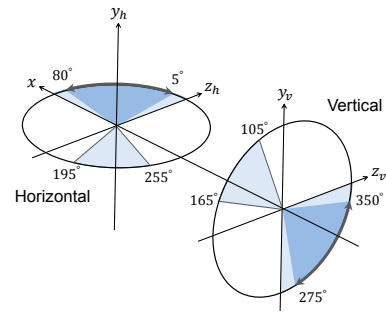


Fig. 6. Verified Motion Range in  $z$ - $x$  Plane and  $z$ - $y$  Plane

TABLE I  
PARAMETERS OF THE MECHANISM

$\theta$ : motion range [deg]	75
$d$ : distance between $O$ and $O'$ [mm]	14.4
$r_1$ : radius of the rotor [mm]	6
$r_2$ : radius of the ratchet gear [mm]	9.45
$\alpha$ [deg]	17.5
$\beta$ [deg]	14.4

movement. As the figure shows, the pendulum movement can be made in the region of 105 - 165 deg and 270 - 360 deg in  $z$ - $y$  plane and 0 - 90 deg and 195 - 255 deg in  $z$ - $x$  plane. The developed robotic system performs within 75 deg, shown by dark blue areas shown in Fig. 6, for its motion range, and it can make a more stable rotation in the selected motion range compared to the other areas. It is difficult to make rotation of over 80 deg without switching the sequence, and it takes about 20 seconds for changing the sequence which makes the system less practical.

##### B. 2-Axis Motion Verification

The parameters for the mechanism were determined from the rotation range selected from the experiment on section IV-A. Table I presents each parameters of the proposed mechanism. The number of the ratchet gear's cogs should be selected from parameter  $\beta$ , which represents the amount of rotation of the ratchet gear caused by one stroke of the rotor. The number of cogs is calculated by  $360/2\beta$ . In this study, the number of cogs was set to 10.

This experiment was conducted in order to verify the movement of the actuator units and to realize multiaxial movement by controlling the gradient field. Fig. 7 shows the developed actuator units and actual condition of the experiment. Table II shows the elements of the sequence used to move the rotor. To realize the pendulum movement, direction of the slice-selective gradient was switched every 1.8 seconds in this sequence. Also, the direction of the gradient was adjusted to get the strongest force at the moment the rotor and the ratchet gear make contact.

The experiment was conducted under two conditions, with and without the rack gear. Fig. 8 shows the timing chart that gives relationship between time and rotation of the rotor under these conditions. The two actuator units can be driven independently. However, the chart also shows that

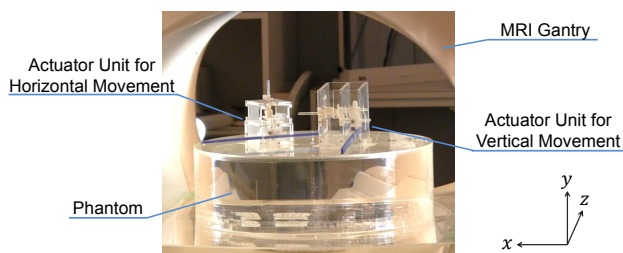


Fig. 7. Developed Actuator Units and Actual Condition of the Experiment

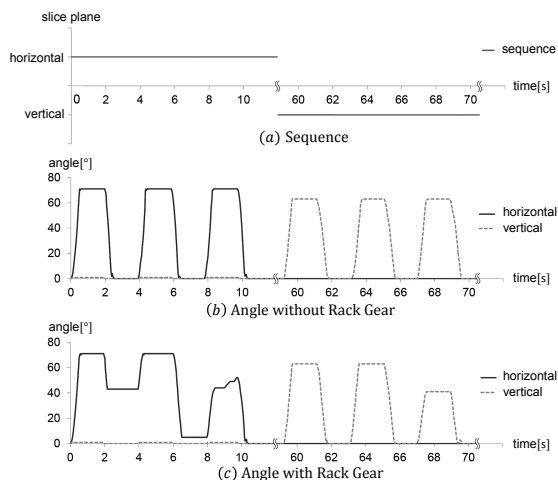


Fig. 8. Timing Chart of Sequence and Output Rotation Angle with and without a Rack Gear

the rotation of the rotor is not stable with rack gear. From prior investigations, it was already discovered that 0.02 N is needed to activate the rotor without rack gear and 0.07 N is needed to activate the rotor with rack gear. We assume that the reason of the unstable movement of the rotor is that the force applied to the ferromagnetic sphere was not enough for moving the mechanism with rack gear.

Fig. 9 shows the position relationship between the two actuator units and the direction of the gradient field. In the figure, A, B, C, and D shows slice-selective angles of the gradients needed to move the rotor from each position:  $\alpha_v$ ,  $\beta_v$ ,  $\alpha_h$ , and  $\beta_h$ , respectively. The direction of slice-selective gradient will be perpendicular to the angle.

While repeating the trials, both actuator units started to activate simultaneously at some point. By observing each axis direction element of the gradients shown in Fig. 9, it can be seen that there are some situations in which both rotors will receive magnetic force. We consider that the ferromagnetic spheres could be magnetized during the trials, making the force stronger as the rotor moved. The force generated to non-targeted rotor is quite small and it cannot move even the ratchet gears.

From these results we verify the feasibility of a MR-compatible robotic system with two-axis movement.

## V. CONCLUSIONS

This paper introduced a novel MR-powered robotic system that can be activated by the gradient field generated from a

TABLE II  
PARAMETERS OF TURBO SPIN ECHO

Repetition Time (TR) [ms]	878
number of slice	5
slice thickness [mm]	0.5
slice-selective angle [deg]	-40, 40

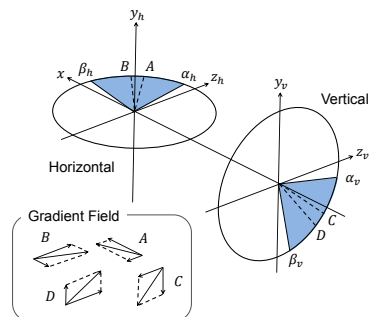


Fig. 9. Position Relationship Between Two Actuator Units

MRI scanner. We have developed modular robotic system, and achieved multiaxial movement that can be controlled by an existing imaging sequence, TSE.

The potential application of this system includes MRI-guided needle biopsy. By using the robotic system, it is possible to make the inspections automated. For future works, it is necessary to increase the torque by improving the mechanism, such as by changing the gear ratio. Furthermore, the relationship between magnetization and the number of times the sequence is applied should be studied to clarify and better control the behavior of the system.

## REFERENCES

- [1] K. E. Peyer, L. Zhang, B. J. Nelson, Bio-inspired magnetic swimming microrobots for biomedical applications, *Nanoscale*, 5(4): 1259-1272, 2013.
- [2] S. Schuerle, S. Erni, M. Flink, B. E. Kratochvil, B. J. Nelson, Three-Dimensional Magnetic Manipulation of Micro- and Nanostructures for Applications in Life Sciences, *IEEE Transactions on Magnetics*, 49(1): 321-330, 2013.
- [3] O. Mori, S. Yabukami, O. Ishii, H. Kanetaka, T. Ozawa, S. Hashi, Position sensing system using magnetic ribbon type marker, *Journal of the Magnetics Society of Japan*, 36(3): 239-244, 2012.
- [4] E. Morita, N. Ohtsuka, Y. Shindo, S. Nouda, T. Kuramoto, T. Inoue, M. Murano, E. Umegaki, K. Higuchi, In vivo trial of a driving system for a self-propelling capsule endoscope using a magnetic field, *Gastrointestinal endoscopy*, 72: 836-840, 2010.
- [5] H. Sajima, H. Kamiuchi, K. Kuwana, T. Dohi, and K. Masamune, MR-Safe Pneumatic Rotation Stepping Actuator, *Journal of Robotics and Mechatronics*, 24(5): 820-827, 2012.
- [6] T. Aodai, S. Toyama, Development of MRI Compatible Manipulandum for Hand and Arm Movement, *Journal of Robotics and Mechatronics*, 21(1): 20-27, 2009.
- [7] R. Moser, R. Gassert, E. Burdet, L. Sacher, H.R. Woodtli, J. Erni, W. Maeder, H. Bleuler, An MR compatible robot technology, *IEEE Int. Conf. on Robotics and Automation*, pp. 670-675, 2003.
- [8] Panagiotis Vartholomeos, Lei Qin, Pierre E. Dupont, MRI-powered Actuators for Robotic Interventions, *IEEE Int. Conf. Intelligent Robots and Systems*, pp. 689-694, 2012.
- [9] P. Vartholomeos, C. Bergeles, L. Qin, P. E. Dupont, Closed-Loop Control of an MRI-Powered Biopsy Robot, *The Hamlyn Symposium on Medical Robotics*, 2012.
- [10] C. Bergeles, P. Vartholomeos, L. Qin, P. E. Dupont, Closed-Loop Commutation Control of an MRI-Powered Robot Actuator, *IEEE Int. Conf. on Robotics and Automation*, pp. 690-695, 2013.